Published in final edited form as:
IEEE J Biomed Health Inform. 2014 March ; 18(2): 484–491. doi:10.1109/JBHI.2013.2281774.

Modeling Cell–Cell Interactions in Regulating Multiple Myeloma Initiating Cell Fate

Tao Peng,
Department of Radiology, The Methodist Hospital Research Institute and Weil Cornell Medical College, Houston, TX 77030 USA

Huiming Peng,
Department of Radiology, Wake Forest University Health Science, Winston-Salem, NC 27157 USA

Dong Soon Choi,
Methodist Cancer Center, The Methodist Hospital, Houston, TX 77030 USA

Jing Su,
Department of Radiology, Wake Forest University Health Science, Winston-Salem, NC 27157 USA

Chung-Che (Jeff) Chang, and
Department of Pathology, Florida Hospital, Orlando, FL 32803 USA

Xiaobo Zhou
Department of Radiology, Wake Forest University Health Science, Winston-Salem, NC 27157 USA

Tao Peng: taop@uci.edu; Huiming Peng: hpeng@wakehealth.edu; Dong Soon Choi: dchoi@tmhs.org; Jing Su: jsu@wakehealth.edu; Chung-Che (Jeff) Chang: jeffchang@pol.net; Xiaobo Zhou: xizhou@wakehealth.edu

Abstract

Cancer initiating cells have been documented in multiple myeloma and believed to be a key factor that initiates and drives tumor growth, differentiation, metastasis, and recurrence of the diseases. Although myeloma initiating cells (MICs) are likely to share many properties of normal stem cells, the underlying mechanisms regulating the fate of MICs are largely unknown. Studies designed to explore such communication are urgently needed to enhance our ability to predict the fate decisions of MICs (self-renewal, differentiation, and proliferation). In this study, we developed a novel system to understand the intercellular communication between MICs and their niche by seamlessly integrating experimental data and mathematical model. We first designed dynamic cell culture experiments and collected three types of cells (side population cells, progenitor cells, and mature myeloma cells) under various cultural conditions with flow cytometry. Then we developed a lineage model with ordinary differential equations by considering

Correspondence to: Xiaobo Zhou, xizhou@wakehealth.edu.

T. Peng, H. Peng, and D. S. Choi contributed equally to this work.
He is now with the Department of Mathematics, University of California, Irvine, CA 92697 USA

This paper has supplementary material available: at http://ieeexplore.ieee.org provided by the authors.

secreted factors, self-renewal, differentiation, and other biological functions of those cells, to model the cell–cell interactions among the three cell types. Particle swarm optimization was employed to estimate the model parameters by fitting the experimental data to the lineage model. The theoretical results show that the correlation coefficient analysis can reflect the feedback loops among the three cell types, the intercellular feedback signaling can regulate cell population dynamics, and the culture strategies can decide cell growth. This study provides a basic framework of studying cell–cell interactions in regulating MICs fate.

Index Terms

Cancer initiating cell; lineage model; mathematical modeling; multiple myeloma (MM); parameter estimation

I. Introduction

Multiple myeloma (MM) is the second most common hematologic malignancy, with about 15,000 new cases per year in USA, and remains incurable with a median survival of 3–5 years even with recently developed novel therapeutic agents and high dose chemotherapy with autologous stem cell transplantation [1]. Failure of myeloma cells to undergo apoptosis plays an important role in the accumulation of myeloma cells within the bone marrow. Several anti-apoptotic proteins and anti-apoptotic signaling cascades have been identified that contribute to the survival of the myeloma [1], [2]. Actually, adhesion of MM cells to bone marrow stromal cells (BMSCs) upregulates cytokine secretion from both BMSCs and tumor cells, and then triggers cytokine-mediated tumor cell growth, survival, drug resistance, and migration.

It has become clear that many cancers, including MM, arise from a small population of cancer stem cells that retain key stem cell properties, including self-renewal, to drive tumorigenesis. The presence of myeloma stem cells or myeloma initiating cells (MICs) is relatively well documented in the pioneer works by Matsui *et al*. [3], [4], compared to most types of cancers. Previous studies have suggested that CD138+ mature myeloma cells cannot give rise to clonogenic MM growth *in vitro* but a small amount of CD138−B cells can [3]. These cells present in myeloma patient blood samples or myeloma cell lines possessing the characteristics shared by stem cells, i.e. they can be identified by Hoechst side population (SP) and positive Aldefluor assay [4]. Studies have shown that well-known chemotherapeutics (dexamethasone, lenalidomide, bortezomib, and 4-hydroxycyclophosphamide) inhibit CD138+ mature myeloma cells but had little effect on MICs *in vitro* [4]. The earlier experimental findings agree with the clinical observation that many agents are active in killing MM cells, but majority of the patients relapse, likely due to regrowth of residual MICs. SP is a phenotype on flow cytometry, originally characterized in murine hematopoietic stem cells, but is now described to be a feature of many different stem cell populations [5]. In this study, we propose to use SP as the marker to select MICs.

Although MIC may hold many properties of normal stem cells, the underlying mechanism of MIC development is largely unknown, and even the identification and purification of MIC from tumor is a challenge. Hence novel methods and biomarkers used to label and

isolate MIC will be of great importance for further MIC studies and, subsequently, cancer therapy. Furthermore, the proliferation and differentiation of MIC will significantly affect the tumor growth, evolution, and heterogeneity as well. Therefore, understanding and quantitatively modeling the patterns of MIC commitment at cellular level and the mechanisms of modulating MIC fate at molecular level will enhance our ability to predict the tumor development, treatment outcomes, and novel therapy strategies.

Studies have suggested that the MICs may play an important role in supporting MIC lineage and that targeting MIC lineage is an attractive therapeutic approach for curing MM. However, the study of MIC linage is currently hampered by the lack of *in vitro* and *in vivo* models suitable for evaluating this interaction. We will use the model established in this study to start answering some fundamental questions about this interaction such as apoptosis (survival), proliferation, and differentiation of various stages of MM cells, i.e., MICs, progenitor cells (PCs), and mature myeloma cells (MCs), as well as secreted inhibitory and stimulatory factors. In our developed model, we incorporate different stages of MM cell development and consider self-renewal and differentiation for MM cells. In addition, the model also includes the feedbacks between different types of cells during MM cell development, which is regulated by stimulation/inhibition factors, such as various cytokines secreted by diverse types of cells. The purpose of this study is to take advantage of our expertise in cell biology and computational modeling to develop coherent experimental protocols and construct mathematical models for understanding the mechanism underlying MIC evolution from subcellular level to cellular level.

The rest of this paper is organized as follows. In Section II, we present the cell culture procedure and the experimental data. Based on these data, a mathematical model to simulate the cell–cell interactions as well as the MM cell growth are constructed in Section III, and then some theoretical results predicted from the model are shown in Section IV. Finally, we present some discussions and conclude the paper in Section V.

II. Cell Culture and Experimental Data

A. Hoechst Side Population Analysis and Cell Culture

Hoechst staining was performed according to the protocol outlined by the Goodell's lab at the Baylor College of Medicine. Briefly, human MM Roswell Park Memorial Institute (RPMI) 8226 cells were harvested by centrifuge and washed in PBS, and then re-suspended at 1×10^6 cells/mL in Dulbecco's Modified Eagle Medium (DMEM) supplemented with 10 mM HEPES (Invitrogen) and 2% FBS with Hoechst 33342 dye at a final concentration of 10 g/mL. After incubation at 99 °F for 60 min, the cells were centrifuged and re-suspended in cold Hanks' balanced salt solution (HBSS) buffers with 2 g/mL propidium iodide (PI) to exclude dead cells. Sample was then put on ice before sorting. Hoechst dye was then excited with UV laser at 350 nm and signal measured with Hoechst blue and Hoechst red filters. SP cells were sorted out by cell sorter and used for further experiments. The collected SP cells were then cultured as explained later.

As summarized in Fig. 1(a), the SP cells were sorted and cultured in RPMI 1640 (10% FBS) for four days and then 80% of cells were resorted for the SP cells. The remaining 20% of the

cells were then separated into two groups, i.e., “nonsorted & old medium (NSOM)” (1/2 of the old medium and 1/2 of fresh RPMI 1640 plus 10% FBS) and “nonsorted & new medium (NSNM)” (fresh RPMI 1640 plus 10% FBS), for further SP analysis at Day 9 and Day 14. The resorted SP cells were also divided similarly as earlier into two groups, i.e., “sorted & old medium (SOM)” and “sorted & new medium (SNM)”, for further SP analysis at Day 9 and Day 14. Before the SP analysis, the total cells were stained with CD138-PE as a marker for cell differentiation from SP cells to PCs (CD138− non-SP cells) or MCs (CD138+ non-SP cells).

The results indicated that when sorted SP cells were cultured for four days, most of progenies were committed to PCs or MCs with only 2.17% SP cells remaining. Additionally, SP cells continued to decline at Day 9 to only 0.83% under the condition of NSNM, while most cells died at Day 9 under the condition of NSOM [data thus not shown in Fig. 1(a)]. Similarly, the resorted SP cells shown significant declining of SP cells with old medium compared to replacing new medium at Day 4. These findings suggest that the differentiated cells may secret inhibitory factors to inhibit the development of MM cells. In addition, Fig. 1(b) shows two examples of the flow cytometry data under conditions of SNM at Day 9 and SOM at Day 9.

III. Mathematical Model Construction

A. Lineage Model of MIC, PPC, CPC, and MC

The hematopoietic hierarchy can be divided into a number of discrete compartments [see Fig. 2(a)] from MICs to fully differentiated MCs. Each compartment can be viewed as representing a cell population at a distinct state of maturation, with unidirectional transition between compartments. Our previous study [6] showed that MIC may undergo self-renewal and differentiation. A cell population can be constructed based on each compartment of the lineage model, in which the number of cells depends on the number of cells entering from the earlier compartment, the cell proliferation rate, and the probability of self-renewal.

As it is described in Fig. 2(b), the MICs can self-renew or differentiate to primitive PCs (PPCs) and committed PCs (CPCs), and the CPCs also can self-renew or differentiate to MCs, and MCs can proliferate by themselves. In addition, apoptosis will be considered in the stage of MC [7].We consider several compartments during the MIC development as modeled in [8]–[10]. The major purpose is to elucidate the dynamic changes of the numbers of these four cell types during MIC development.

As we can see from Fig. 2(a), X_1 represents the number of MICs, X_1 to X_{10} represent the number of PPCs in each compartment for the process of progenitor development, X_1 to X_{12} represent the number of CPCs in each compartment for the process of progenitor development, andX_{13} toX_{18} represent the number of MCs in each compartment, respectively. We denote f_i as the probability of self-renewal of MM cells in the ith compartment. μ_i represents the proliferation rate of MM cells in the ith compartment; d_{MC} represents the apoptosis rate of MCs. We ignore the apoptosis terms for MICs, PPCs, and CPCs [see (1)–(2)], because the apoptosis rates are rather small in those stages. Therefore, by referring to

[8]–[10], an ordinary differential equations (ODEs) system of the lineage model for MIC development can be constructed as follows:

$$\frac{dX_1}{dt}=(2f_1-1)\mu_1 X_1 \quad (1)$$

$$\frac{dX_i}{dt}=2(1-f_{i-1})\mu_{i-1}X_{i-1}+(2f_i-1)\mu_i X_i \quad (2)$$

$$\frac{dX_i}{dt}=2(1-f_{i-1})\mu_{i-1}X_{i-1}+(2f_i-1)\mu_i X_i - d_{\mathrm{MC}}X_i. \quad (3)$$

Note that the range of *i* is from 2 to 12 in (2) and from 13 to 18 in (3). This lineage model is a deterministic model, which describes the growth of MM cancer cells at different stages. It is worth noting that, although this type of lineage model of stem cell development has been well established in literature such as [8]–[10], none of them has paid attention to the MIC development, which is the focus of our work. For example, [8] focused on neural stem cell, [9] hematopoietic stem cell, and [10] mesenchymal stem cell. Next we will focus on the determination of the major parameters in the lineage model, which include self-renewal probabilities and proliferation rates, by linking them to the secreted factor system.

B. Secreted Factor System

In order to completely build the mathematical model for the considered MICs development system, we design a secreted factor system to describe how the different cell compartments interact with each other, how the factors are secreted from cells at different stages, and how the major system parameters in the lineage model are determined by the secreted factors. Fig. 2(b) gives us an intuitive diagram for this system, where SSF1 and SSF2 represent secreted stimulatory factors that are able to stimulate the survival of MM cells and ISF1 and ISF2 represent secreted inhibitory factors that are able to inhibit the survival of MM cells. Briefly, SSF1 produced by MCs stimulates the self-renewal of MM cells, SSF2 produced by MCs stimulates the proliferation of MM cells, ISF1 produced by MCs inhibits the proliferation of MM cells, and ISF2 produced by PPCs inhibits the self-renewal of MM cells. The secreted factors used here represent the general relationship of different known or unknown molecules instead of some specific molecules. The major reason of the usage of the general representation is because the secreted factors remain largely theoretical and most of them are still needed to be identified by research in the future though some potential candidates have been identified in the literatures. For example, TGF-β is a well-established inhibitor of stem and progenitor expansion *in vitro* and *in vivo* [7], IL-8 suppresses myeloid colony formation *in vitro* [11], a few molecules with stimulatory effects on self-renewal and proliferation have been reported as being expressed by hematopoietic cells [9].

Then, by referring to [9], we model the secreted factor system as ODEs (4)–(7) with Hill-type functions to describe the feedback loops shown in Fig. 2(b)

$$\frac{d[\mathrm{SSF1}]}{dt}=sr_1\cdot\frac{(\mathrm{nMC}/D_1)^{d_1}}{1+(\mathrm{nMC}/D_1)^{d_1}} \quad (4)$$

$$\frac{d[\mathrm{SSF2}]}{dt}=sr_2\cdot\frac{(\mathrm{nMC}/D_1)^{d_1}}{1+(\mathrm{nMC}/D_1)^{d_1}} \quad (5)$$

$$\frac{d[\mathrm{ISF1}]}{dt}=sr_3\cdot\frac{(\mathrm{nMC}/D_1)^{d_1}}{1+(\mathrm{nMC}/D_1)^{d_1}} \quad (6)$$

$$\frac{d[\mathrm{ISF2}]}{dt}=sr_4\cdot\frac{(\mathrm{ISF1}/L_s)^{K_s}+(\mathrm{nCPC}/D_2)^{d_2}}{1+(\mathrm{ISF1}/L_s)^{K_s}+(\mathrm{nCPC}/D_2)^{d_2}}. \quad (7)$$

Note that Hill-type functions are used herein to substitute for the linear functions proposed in [9], for Hill-type function is more reasonable to describe a certain growth from a biological point of view. In this system, nMC denotes the number of MCs given by the sum of X_{13} to X_{18}; nCPC denotes the number of CPCs given by the sum of X_1 to X_{12}; the parameters are described in Table I. Finally, we complete the lineage model by linking together with the secreted factor system and using algebra equations incorporating with Hill-type functions as well as Gaussian-type functions to describe the self-renewal probabilities and proliferation rates as (8)–(10)

$$f_i=f_{\max}\cdot e^{-(i-1)^2/(2D_{\mathrm{SR}}^2)}\cdot\frac{1+(\mathrm{SSF1})^{k_1}}{1+(\mathrm{ISF2})^{k_4}+(\mathrm{SSF1})^{k_1}} \quad (8)$$

$$\mu_i=\mu_{\max}\cdot e^{-(i-n_{\max})^2/(2D_{\mathrm{GR}}^2)}\cdot\frac{t^{k_t}}{\tau_D^{k_t}+t^{k_t}}\cdot\frac{1+(\mathrm{SSF2})^{k_2}}{1+(\mathrm{ISF1})^{k_3}+(\mathrm{SSF2})^{k_2}} \quad (9)$$

$$\mu_i=\mu_+\cdot\frac{t^{k_t}}{\tau_D^{k_t}+t^{k_t}}\cdot\frac{1+(\mathrm{SSF2})^{k_2}}{1+(\mathrm{ISF1})^{k_3}+(\mathrm{SSF2})^{k_2}}. \quad (10)$$

Note that the range of *i* is from 1 to 18 in (8) and from 1 to 12 in (9) and from 13 to 18 in (10). It is important to note that we build the earlier algebra equations by referring to [9] meanwhile transforming the Eq. (16)] in [9] into two equations (9) and (10) herein to distinguish between the two cases of CPC and MC. In the earlier equations, τ_D denotes the time for 50% of the cells to enter cycle and k_t denotes the Hill coefficient defining the rate at which cells are induced to cycle and here we set τ_D = 2 days and k_t = 4 as previously described [9], and the other parameters are described in Table I.

C. Parameter Estimation

The resulting model as described through (1)–(10) contains 21 unknown parameters shown in Table I. Dynamic data from experiment shown in Fig. 1(a) was used as a training set to estimate those parameters through a reverse engineering strategy. The objective function, which is based on the errors between theoretical and experimental data, is defined as follows:

$$J(\Theta)=\sum_{i=0}^{I-1}\sum_{j=1}^{J_t}\omega_i\left\|V^{(\mathrm{th})}(\Theta;t_j^{(i)})-V^{(\mathrm{exp})}(t_j^{(i)})\right\|^2. \quad (11)$$

In the earlier objective function, $\|\cdot\|$ denotes the L^2 norm operator; $\Theta=(\theta_1, \theta_2, \ldots, \theta_{21})$ denotes the vector of parameters in the lineage model; Ω is the available parameter space; I represents the number of experimental stages that is set as $I = 4$; J_i represents the number of time points of observation for ith stage of experiment; $t_j^{(i)}$ represents the jth time points of observation in the ith stage; and ω_i represents the corresponding coefficients of the weights in the four different stages, and here we set all of them as 1 equally based on the experimental conditions and model assumptions. There is one time point for the first two stages of experiments, two time points for the last two stages of experiments, and the corresponding parameters are set as $J_0=1, t_1^{(0)}=4, J_1=1, t_1^{(1)}=9, J_i=2, t_1^{(i)}=9, \mathrm{and} t_2^{(i)}=14$ for $i = 2, 3$. In addition, the two variables, $V^{(\mathrm{th})}$ and $V^{(\mathrm{exp})}$ represent the theoretical and experimental vectors of the observations composed of three types of cells, i.e., V = (pSP, pPC, pMC), where pSP, pPC, and pMC denote the percentages of SP cells, PCs, and MCs over the total cells (TCs).

Finally, a total of 18 system outputs (experimental data) are therefore used to fit 21 model parameters listed in Table I by minimizing the earlier objective function, namely

$$\Theta^*=\arg\min_{\theta\in\Omega} J(\Theta). \quad (12)$$

Because of the highly nonlinear and multi-modal nature of the objective function (J), the multi-scale algorithm based on Particle Swarm Optimization (PSO) [12], [13] was used to solve this nonlinear programming problem. The whole algorithm included the following three steps. The first step is to determine the rough searching range. Because the model was built using biological knowledge, the involved parameters had the corresponding biological meanings. Accordingly, we could get the rough searching range. The second step is to globally search the optimal solution on the scale of $10^{\Theta 1}$ (Θ_1 is the optimized vector). Because of the limitation of PSO, we search the optimal solutions 20 times independently and choose the best one. The third step is to locally search the optimal solution on the scale of Θ_2 (Θ_2 is the optimized vector). PSO was employed to search the optimal solution.

The final results of parameter estimations are shown in Table I, and the corresponding fitting results are shown in Fig. 3(a)–(c). Most of the fitting errors are rather small except for those under the condition of SNM at Day 14 shown in Fig. 3(a). There may be several reasons

causing this problem. First, we only considered four secreted factors in our model, SSF1, SSF2, ISF1, and ISF2. However, in the intercellular environment there are many factors that are involved in the self-renewal, differentiation, and proliferation of different MM cells. Second, the signaling pathways related to the secreted factors were not considered. In other words, the lineage model is still a simplified model. We hope that the combination of the lineage model and signaling pathway model will provide more detailed simulation of cell development in the future research.

D. Parameter Identifiability and Sensitivity Analysis

Coefficient of variation (CV) based on bootstrapping approach [14] was used to study whether and how many parameters are identifiable. CV is a normalized measure of dispersion of a probability distribution of a variable, which is defined as the ratio of the standard deviation to the mean. Briefly, we first resampled the experimental data for 100 times using bootstrapping approach. Then, based on the resampled data, we obtained 100 sets of estimated parameters using the proposed optimization algorithm. Finally, based on the estimated parameters sets, we calculated the CVs for all parameters and defined the number 1 as the threshold to determine the identifiability for parameters. The results are shown in Table I, in which the CVs marked with red color illustrate the corresponding parameters are nonidentifiable and thus about 76% of the parameters are identifiable in our model.

Parameter sensitivity analysis is a tool to quantitatively determine the effect of specific parameters on the output. To understand the relationship between system responses and variations in individual model parameters, local parameter sensitivity analysis was performed (see [15] for detail). Briefly, we increased or decreased the estimated value of each parameter by 1% and then checked the response of the system outputs in order to determine the corresponding parameter sensitivity. In Fig. 3(d)–(i), the results show the percentage changes of system outputs are less than 6% for most all parameters as increased or decreased by 1%, which demonstrates the stability of our model. It is also worth noting that three most sensitive parameters may control the antagonistic relationship between mature and primitive cell compartments, including the 1st parameter $f_{\max}$, the 2nd parameter $n_{\max}$, and the 19th parameter D_1 as it has been shown that the regulation of stem cell self-renewal and proliferation plays an important role in preventing cancer cells [16].

E. Model Cross-Validation

Here we use cross-validation to evaluate how accurately our model will perform. In the cross-validation technique, we first partitioned the observations into two complementary subsets, and then used one subset to train the model and the other to test and validate the model. In our study we used leave-one-out cross-validation. That means we used one single observation from original sample as the validation data and the remaining observations as the training data. This process was repeated until each observation in the dataset was used once as the validation data. The results are shown in Fig. 4.

Briefly, we first got the estimated parameters of the lineage model based on the whole dataset, and the estimated parameters of the lineage model based on the dataset in which one

single observation is deleted. Then we calculated the relative errors (REs) for all parameters by comparing these two sets of estimated parameters. The results are presented in Fig. 4(a) where we can see that the RE is rather large for the 8th parameter μ_+ and the 20th parameter D_2 .

Fig. 4(b)–(d) shows the comparison results between the experimental data and the predicted outputs from the estimated model trained by the leave-one-out dataset. About 94% of results are consistent with the experimental data. For example, when we leave out the single data of "the percentage of PCs at Day 9 under the condition of SNM" from the whole dataset, the predicted data from the model trained by the leave-one-out dataset does not show a good agreement with the experimental data, as shown in Fig. 4(c). This happens may be due to the following reasons. First, the size of the whole dataset is not big enough, hence when we leave one out of the dataset, some important information such as nonlinear property could be lost. Second, we did not consider signaling pathways in the different types of cells in the lineage model, which could make the model inaccurate in cell population prediction. Generally speaking, our model can be used to do the prediction in practice because only one out of 18 cases did not show good performance.

IV. Theoretical Results

A. Correlation Coefficient Analysis Reflects Feedback Loops

To systematically explore the regulation function of the model parameters in an unbiased manner, the Pearson correlation coefficients (PCCs) were employed to investigate the relationships between 21 model parameters and 18 system outputs. The detailed method for the calculation of PPCs in the simulation is provided in the supplementary.

The results are presented using a heat map shown in Fig. 5. First, the results show the strong correlations between the 2nd parameter n_{ma} and most of the model outputs, which means that the parameter n_{max} plays an important role in regulating MICs development. Second, the 4th parameter D_{GR} shows strong negative correlations with the outputs of the percentages of SP under all cultural conditions. Third, the outputs of the percentages of MCs under all cultural conditions have strong correlations with all parameters. Finally, the correlation is significantly negative between the 19th parameters D_1 and the 14th output (the percentage of PCs under the condition of SNM at Day 9), which indicates that the secreted factors produced by MCs have significant effects on regulating the MICs development through the corresponding feedback loops depicted in Fig. 2(b).

B. Intercellular Feedback Signaling Regulates Cell Population Dynamics

Here, we simulated the dynamics of the number of total cells and the percentage of SP in response to different theoretical treatments shown in Fig. 6. In the simulation, the culture in each condition was intermittently renewed (i.e., all secreted factors are reset back to zeros) every two days after Day 4.

First, we considered the treatment of increasing the self-renewal rate (increasing f_{max} by 50%). The simulation results in Fig. 6 show that the number of total cells expands faster and the percentage of SP reaches the steady stage in the same short time period compared to the

control condition, which means that increasing self-renewal rate can only influence the number of total cells but not the percentage of SP. Second, we considered the treatment of partially blocking the differentiation (decreasing μ_{max} by 50%). The results show that the increase of the total cell number slows down and the percentage of SP is rather high compared to the control condition. Third, we considered the treatment of "unresponsive to the promoters" in which the promotion factors do not affect the self-renewal and differentiation (setting SSF1 = SSF2 = 0 in the model). The results show the increase of the total cell number is totally inhibited, i.e., blocking the stimulatory factors can result in inhibiting the growth of cell population, indicating that stimulatory factors play important roles in regulating the MM cell development. From the discussion earlier, we can conclude that stimulatory factors may play a major role in regulating the self-renewal and differentiation of MM cells.

C. Culture Strategies Decide Cell Growth

We also in silico studied the cell culture strategies based on the established linage model by renewing the medium at three different frequencies of culture manipulations, i.e., "1 Day", "2 Days", and "3 Days". Three culture strategies were performed in the simulation as follows. "1 Day": resetting all secreted factors back to zeros every 1 day after Day 4 culture; "2 Days": resetting all secreted factors back to zeros every 2 days after Day 4 culture; "3 Days": resetting all secreted factors back to zeros every 3 days after Day 4 culture.

Fig. 7(a) shows the results of the percentage dynamic of SP cells over total cells, the percentage dynamic of MCs over total cells, and the dynamic of the total cell population, along with three different cultural strategies described earlier. With the culture strategy of "1 Day", the total cell number will reach the steady stage early at the 4th day compared to other two culture strategies. Specially, with the culture strategy of "3 Days", the total cell number expands exponentially. Fig. 7(b) and (c) shows the results of the concentration dynamics of ISF1 and ISF2, respectively, along with three different cultural strategies. Fig. 7(b) shows that the faster the culture frequency, the faster the maximal concentration of ISF1 increases. In addition, the concentration of ISF2 is always rather small through 30 days culture with the culture strategies of both "1 Day" and "2 Days" except that it increases significantly after 25 days culture with the culture strategy of "3 Days", as shown in Fig. 7(c). From the earlier discussion, we conclude that increasing the frequency of culture manipulation can result in inhibiting the growth of cell population. Thus, manipulating the culture strategy may make great contributions to the growth of MM cells.

V. Discussion and Conclusion

The goal of this study is to take advantage of our expertise in cell biology and computational modeling to develop coherent experimental protocols and mathematical models for understanding the cell–cell interactions between MICs, PCs, and MCs regulating MICs evolution. We experimentally measured the dynamic population numbers of different types of cells under various cultural conditions. These data were then employed to construct a mathematical model consisting of the MIC lineage model and the corresponding secreted factor system. Finally the model was used to predict some theoretical results. The theoretical

results showed that stimulatory factors play important roles in regulating the MM cell development and blocking the stimulatory factors can result in inhibiting the growth of cell population, and the increasing frequencies of culture manipulation can also result in inhibiting the growth of cell population. This study provides a basic framework of studying cell–cell interactions in regulating MIC fate. The obtained results from dynamic system may be potentially useful for understanding mechanism of cancer stem cells development, as well as the selection of drug treatments in the chemical therapy by targeting the stem cells.

The main limitation of our wok is that we did not consider the signaling pathways involved in the lineage model, though recent studies have suggested that many pathways may be involved in regulating the cellular behavior of cancer stem cells, e.g., Wnt [17], Notch [18], Hedgehog [19], and so on. Second, although some secreted factors have been identified in literature, we did not specify them in our model and just simply classify them into four classes, i.e., SSF1, SSF2, ISF1, and ISF2. Third, we only used the percentages of SP cells, PCs, MCs over TCs based on many theoretical assumptions, and the dynamic changes of these cell numbers were not employed in training our model. In addition, more discussions about the parameters in the model are needed, such as the number of compartments belonging to the stages of MIC, PC, and MC. In order to discover new drugs for treating MM, we need more detailed models and more experimental data. In the following work, the significant pathways will be considered in the model, and more experimental data will be measured, such as reverse phase protein array data that measure the phosphorylation levels of the proteins involved in the signaling pathways.

Supplementary Material

Refer to Web version on PubMed Central for supplementary material.

Acknowledgments

The work of X. Zhou was supported in part by NIH 1U01CA166886, NIH 1R01LM010185, NIH 1U01HL111560, TSI-VAMC, and CCCWFU.

Dr. Zhou was recently awarded three NIH R01 grants, two NIH U01 grants, and one DOD grant as a PI. In addition, he and his colleagues have successfully got other 6 NIH R01 grants. He also organized and substantially contributed to the NIH U54 Center for Systems Modeling of Cancer Development funded in 2010.

References

1. Younes H, Leleu X, Hatjiharissi E, Moreau AS, Hideshima T, Richardson P, Anderson KC, Ghobrial IM. Targeting the phosphatidylinositol 3-kinase pathway in multiple myeloma. Clin. Cancer Res. 2007 Jul 1; 13(13):3771–3775. [PubMed: 17606706]
2. Hideshima T, Mitsiades C, Tonon G, Richardson PG, Anderson KC. Understanding multiple myeloma pathogenesis in the bone marrow to identify new therapeutic targets. Nat. Rev. Cancer. 2007 Aug; 7(8):585–598. [PubMed: 17646864]
3. Matsui W, Huff CA, Wang Q, Malehorn MT, Barber J, Tanhehco Y, Smith BD, Civin CI, Jones RJ. Characterization of clonogenic multiple myeloma cells. Blood. 2004 Mar 15; 103(6):2332–2336. [PubMed: 14630803]
4. Matsui W, Wang Q, Barber JP, Brennan S, Smith BD, Borrello I, McNiece I, Lin L, Ambinder RF, Peacock C, Watkins DN, Huff CA, Jones RJ. Clonogenic multiple myeloma progenitors, stem cell properties, and drug resistance. Cancer Res. 2008 Jan 1; 68(1):190–197. [PubMed: 18172311]

5. Goodell MA, Brose K, Paradis G, Conner AS, Mulligan RC. Isolation and functional properties of murine hematopoietic stem cells that are replicating in vivo. J. Exp. Med. 1996 Apr 1; 183(4):1797–1806. [PubMed: 8666936]
6. Feng Y, Wen J, Mike P, Choi DS, Eshoa C, Shi ZZ, Zu Y, Chang CC. Bone marrow stromal cells from myeloma patients support the growth of myeloma stem cells. Stem. Cells Dev. 2010 Sep; 19(9):1289–1296. [PubMed: 20121456]
7. Yamazaki S, Iwama A, Takayanagi S, Eto K, Ema H, Nakauchi H. TGF-beta as a candidate bone marrow niche signal to induce hematopoietic stem cell hibernation. Blood. 2009 Feb 5; 113(6): 1250–1256. [PubMed: 18945958]
8. Ganguly R, Puri IK. Mathematical model for the cancer stem cell hypothesis. Cell Prolif. 2006 Feb; 39(1):3–14. [PubMed: 16426418]
9. Kirouac DC, Madlambayan GJ, Yu M, Sykes EA, Ito C, Zandstra PW. Cell-cell interaction networks regulate blood stem and progenitor cell fate. Mol. Syst. Biol. 2009; 5:293. [PubMed: 19638974]
10. Pivonka P, Zimak J, Smith DW, Gardiner BS, Dunstan CR, Sims NA, Martin TJ, Mundy GR. Model structure and control of bone remodeling: A theoretical study. Bone. 2008 Aug; 43(2):249–263. [PubMed: 18514606]
11. Broxmeyer HE, Kim CH. Regulation of hematopoiesis in a sea of chemokine family members with a plethora of redundant activities. Exp. Hematol. 1999 Jul; 27(7):1113–1123. [PubMed: 10390186]
12. Kennedy J, Eberhart R. Particle swarm optimization. Proc. IEEE Int. Conf. Neural Netw. 1995; 4:1942–1948.
13. Meissner M, Schmuker M, Schneider G. Optimized particle swarm optimization (OPSO) and its application to artificial neural network training. BMC Bioinformatics. 2006; 7:125. [PubMed: 16529661]
14. Kremling A, Fischer S, Gadkar K, Doyle FJ, Sauter T, Bullinger E, Allgower F, Gilles ED. A benchmark for methods in reverse engineering and model discrimination: Problem formulation and solutions. Genome. Res. 2004 Sep; 14(9):1773–1785. [PubMed: 15342560]
15. Peng H, Wen J, Zhang L, Li H, Chang CC, Zu Y, Zhou X. A systematic modeling study on the pathogenic role of p38 MAPK activation in myelodysplastic syndromes. Mol. Biosyst. 2012 Apr; 8(4):1366–1374. [PubMed: 22327869]
16. Orford KW, Scadden DT. Deconstructing stem cell self-renewal: Genetic insights into cell-cycle regulation. Nat. Rev. Genet. 2008 Feb; 9(2):115–128. [PubMed: 18202695]
17. Reya T, Clevers H. Wnt signalling in stem cells and cancer. Nature. 2005 Apr 14; 434(7035):843–850. [PubMed: 15829953]
18. Brennan K, Brown AM. Is there a role for Notch signalling in human breast cancer? Breast Cancer Res. 2003; 5(2):69–75. [PubMed: 12631384]
19. Liu S, Dontu G, Mantle ID, Patel S, Ahn NS, Jackson KW, Suri P, Wicha MS. Hedgehog signaling and Bmi-1 regulate self-renewal of normal and malignant human mammary stem cells. Cancer Res. 2006 Jun 15; 66(12):6063–6071. [PubMed: 16778178]

Biographies

Tao Peng received the B.S. degree in computational mathematics from Wuhan University, Hubei, China, in 2007. He is currently working toward the Ph.D. degree at the University of California, Irvine, USA.

His current research interests include systems biology, computational biology, and machine learning.

Huiming Peng received the B.S. degree from China University of Geosciences, Wuhan, China, in 2002, the M.S. degree from Wuhan University, Wuhan, China, in 2005, and the Ph.D. degree from China University of Geosciences, in 2011, all in mathematics.

Since 2005, he has been a faculty member with the School of Mathematics and Physics, China University of Geosciences. From 2008 to 2010, he was an exchange Ph.D. student with supervisor Dr. Xiaobo Zhou at the Department of Radiology, The Methodist Hospital Research Institute and Weil Cornell Medical College, Houston, TX. He is currently a Postdoctoral Research Fellow with the Department of Radiology, Wake Forest University School of Medicine, Winston-Salem, NC. His current research interests include systems biology and statistical signal processing.

Dong Soon Choi received the B.A. degree from the University of Texas, Austin, TX, USA, in 1996, and the M.S. degree in biological science and the Ph.D. degree in molecular science and technology from Ajou University, Suwon, Korea, in 2002 and 2007, respectively.

From 2007 to 2011, he was a Postdoctoral Research Fellowat the UT MD Anderson Cancer Center and the Houston Methodist Hospital, Houston, TX, USA. Since 2011, he has been a Research Associate at the Houston Methodist Cancer Center, The Houston Methodist Hospital, Houston. His research interests include the biology of cancer stem cells and their interactive nature with cancer microenvironment, currently focusing on epigenetic modification by anticancer drugs and the related drug-resistance mechanism in cancer stem cells and cancer associated stromal cells.

Jing Su received the Ph.D. degree from Biomedical Engineering, Georgia Institute of Technology, Atlanta, USA, and Emory University, Atlanta, GA, USA.

He is currently an Instructor in the Department of Radiology, Wake Forest School of Medicine, Winston-Salem, NC, USA. His current research interests include systems biology, biomedical informatics, and biomaterials.

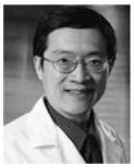

Chung-Che (Jeff) Chang received the M.D. degree from National Yang-Ming Medical College, Taipei, Tiawan, and the Ph.D. degree from Case Western Reserve University, Cleveland, OH, USA.

From 1999 to 2003, he was an Assistant Professor with the Department of Pathology, Medical College of Wisconsin, Milwaukee, WI, USA. From 2003 to 2004, he was an Associate Professor with the Department of Pathology, Baylor College of Medicine, Houston, TX. From 2004 to 2011, he was a Professor with the Department of Pathology, The Methodist Hospital, Houston, TX. Since 2011, he has been a Professor with the Department of Pathology, Florida Hospital, Orlando, USA. His current research interests include clinical and translational, focusing on identifying markers and signaling pathways that are important for diagnosis, prognosis, and treatment of hematological malignancies.

Xiaobo Zhou received the B.S. degree from Lanzhou University, Lanzhou, China, in 1988, and the M.S. and Ph.D. degrees from Peking University, Beijing, China, in 1995 and 1998, respectively, both in mathematics.

From 1988 to 1992, he was a Lecturer with the Training Center, 18th Building Company, Chongqing, China. From 1992 to 1998, he was a Research Assistant and Teaching Assistant with the Department of Mathematics, Peking University. From 1999 to 2000, he was a Senior Technical Manager with the 3G Wireless Communication Department, Huawei Technologies Co., Ltd., Beijing. From 1998 to 2004, he was a Postdoctoral Research Fellow with Tsinghua University, Beijing; the University of Missouri-Columbia; Texas A&M University, College Station; and Harvard Medical School, Boston, MA. From 2005 to 2007, he was a faculty member with Brigham and Women's Hospital and Harvard University, Boston, MA. From 2007 to 2012, he was the Chief of Bioinformatics, Director of Center for Translational Biosystems, Professor of Radiology, The Methodist Hospital, Houston, TX. Since 2013, he has been the Chief of Bioinformatics, the Director of Center for Bioinformatics and Systems Biology, a Full Professor of Diagnostic Radiology, Wake Forest University School of Medicine, Winston-Salem, NC, USA. He and his colleagues pioneered the high-content cellular imaging informatics and the multiscale systems biology.

A

Day 0	Day 4 (before separation)	Conditions	Cell types	Day 4 (after separation)	Day 9	Day 14
500k SPs	2.17% SPs 97.83% PCs & MCs	Non-sorted & New Medium	SP	2.17%	0.83%	
			PC	97.83%	6.26%	
			MC		92.91%	
		Sorted & New Medium	SP	100%	4.42%	5.81%
			PC	0	2.92%	1.91%
			MC		92.66%	92.28%
		Sorted & Old Medium	SP	100%	1.84%	0.40%
			PC	0	1.91%	7.30%
			MC		96.25%	92.3%

B

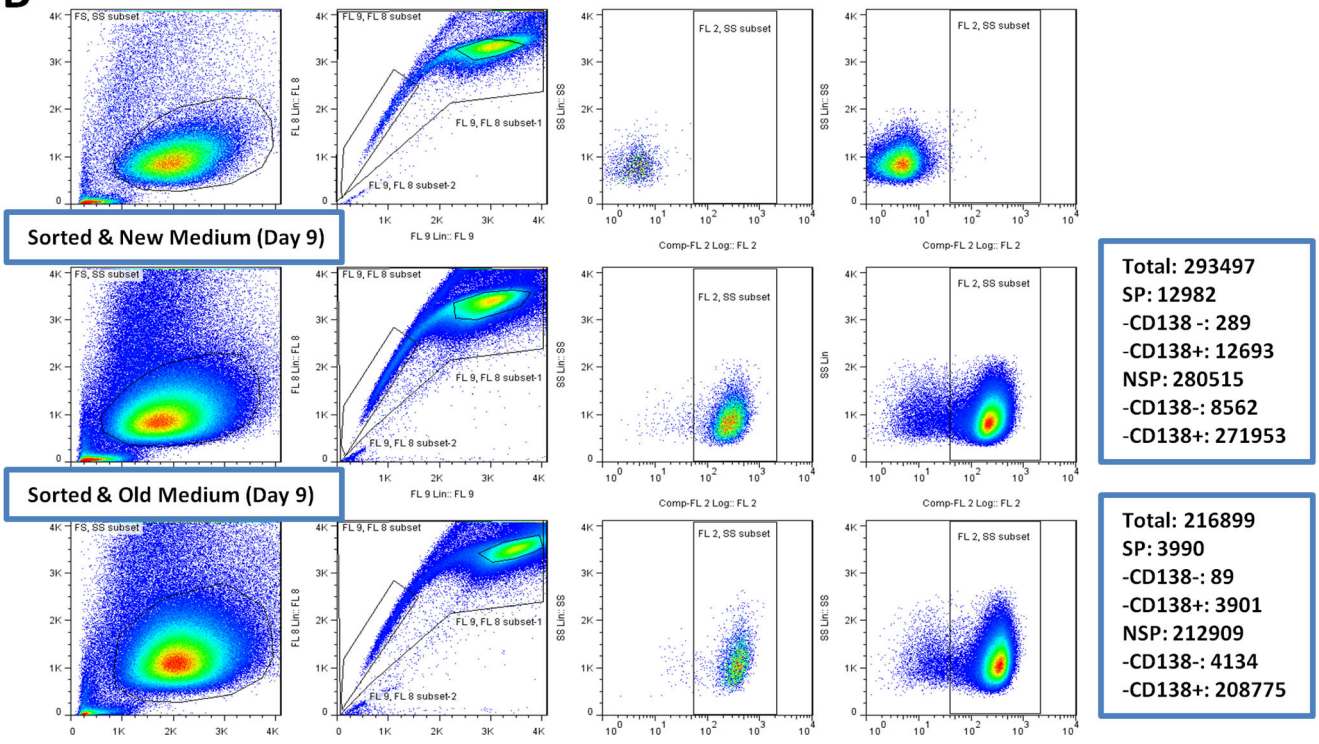

Fig. 1.

Cell culture procedures and experimental data. (a) The flow cytometry data consisting of the percentages of three cell types over the total cells under various cultural conditions. (b) Two examples of the flow cytometry data. The first example shown in the second row is the data under the condition of SNM at Day 9, and the second example shown in the third row is the data under the condition of SOM at Day 9 (the first row is for control condition).

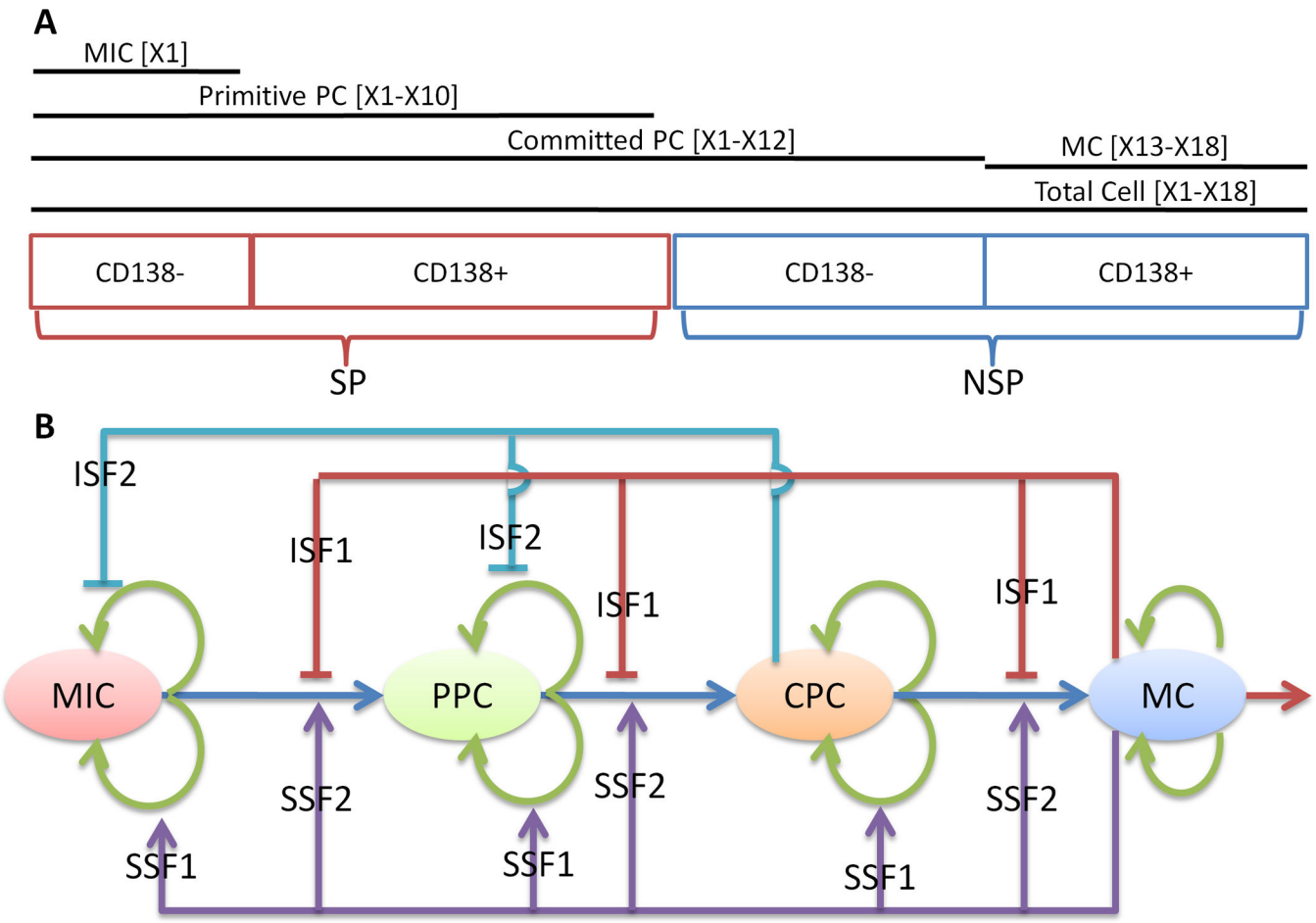

Fig. 2.

Schematic depiction of MICs development model incorporating functional assays and positive and negative feedbacks. (a) The model consists of 18 compartments. SP and non-SP are both composed of CD138− and CD138+. MIC is in the zone of CD138− of SP, PPC is in the zones of CD138− and CD138+ of SP, CPC is in the zones of CD138− and CD138+ of SP and CD138− of non-SP, and MC is in the zones of CD138+ of non-SP. (b) All cells are divided into four types of cells. Each type of cells self-renew. MIC, PPC, and CPC differentiate to PPC, CPC and MC, respectively. MC undergoes the apoptosis. MCs secret SSF1 and SSF2 stimulating the self-renewal and the differentiation respectively, and MCs secret ISF1 inhibiting the differentiation, and CPCs secret ISF2 inhibiting the self-renewal. Note that there is no other meaning of the usage of two green arrows for each self-renew except for the convenience of presentation.

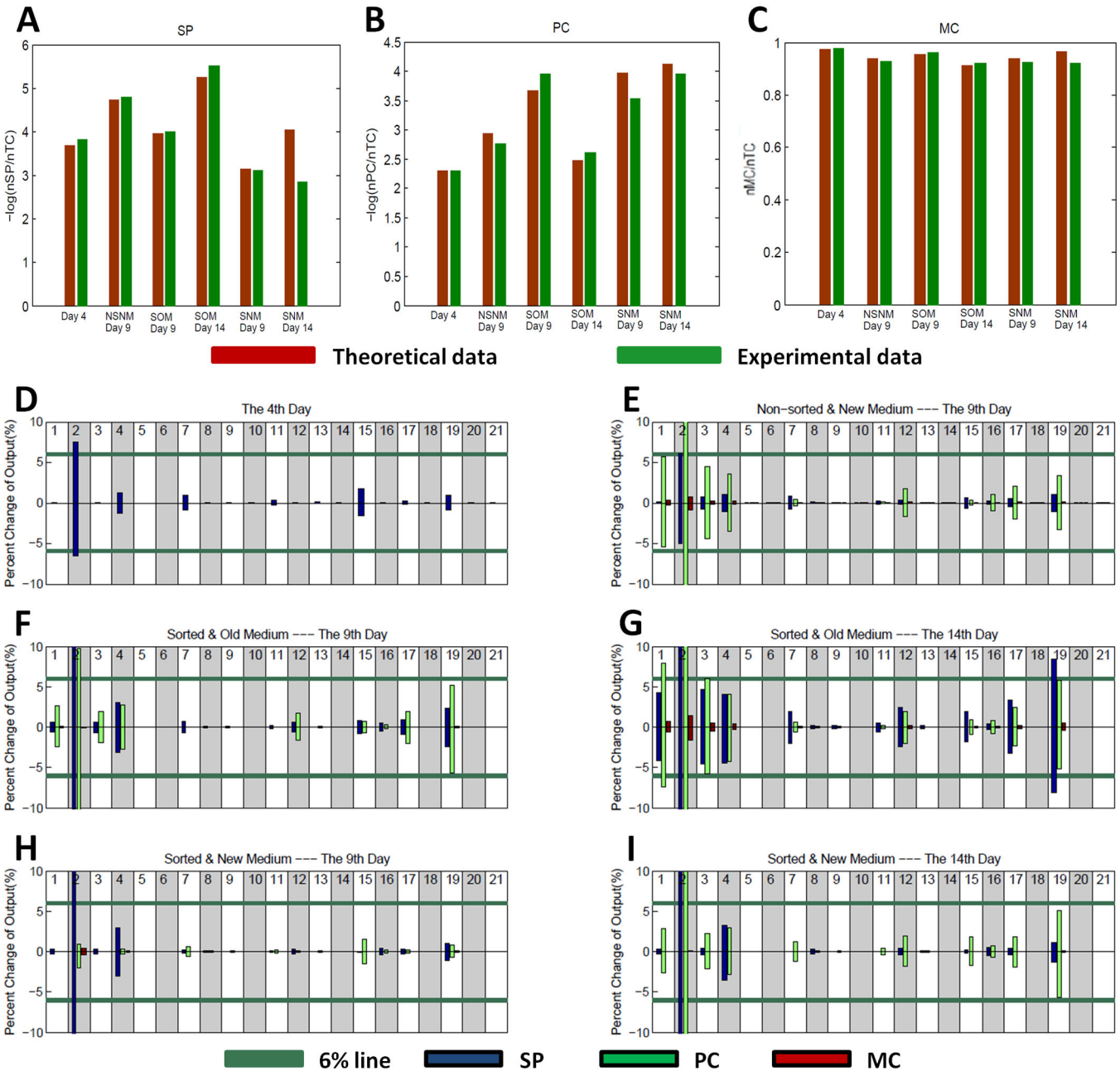

Fig. 3.

Fitting results of parameter estimation and parameter sensitivity analysis. (a–c) The fitting results between theoretical data and experimental data. The brown (left) bar is the theoretical data and the green (right) bar is the experimental data. (d–i) The results of model sensitivity for total 18 system outputs on total 21 kinetic parameters listed in Table I.

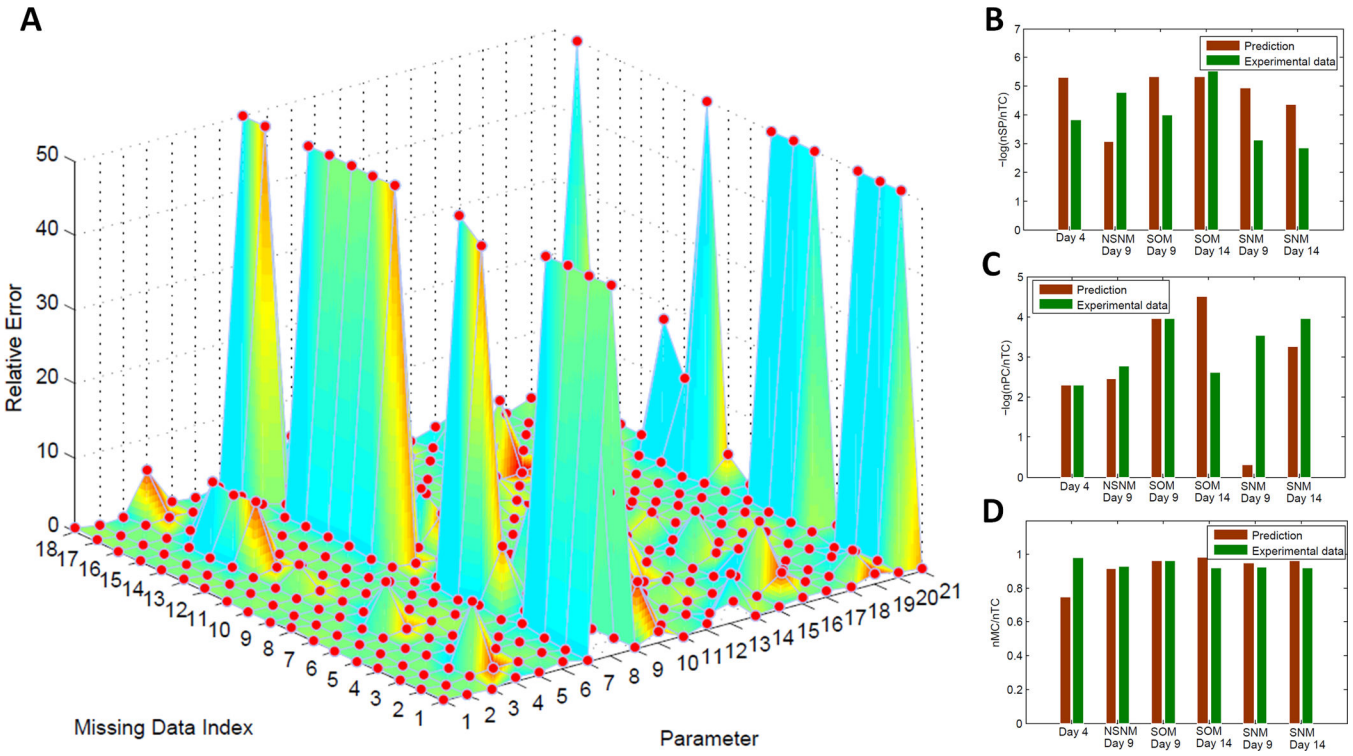

Fig. 4.

Results of leave-one-out cross-validation. (a) The REs between the estimated parameters trained by the leave-one-out datasets and the estimated parameters trained by the whole dataset. (b–d) The comparisons between the experimental data and the theoretical data predicted from the developed model trained by the leave-one-out datasets.

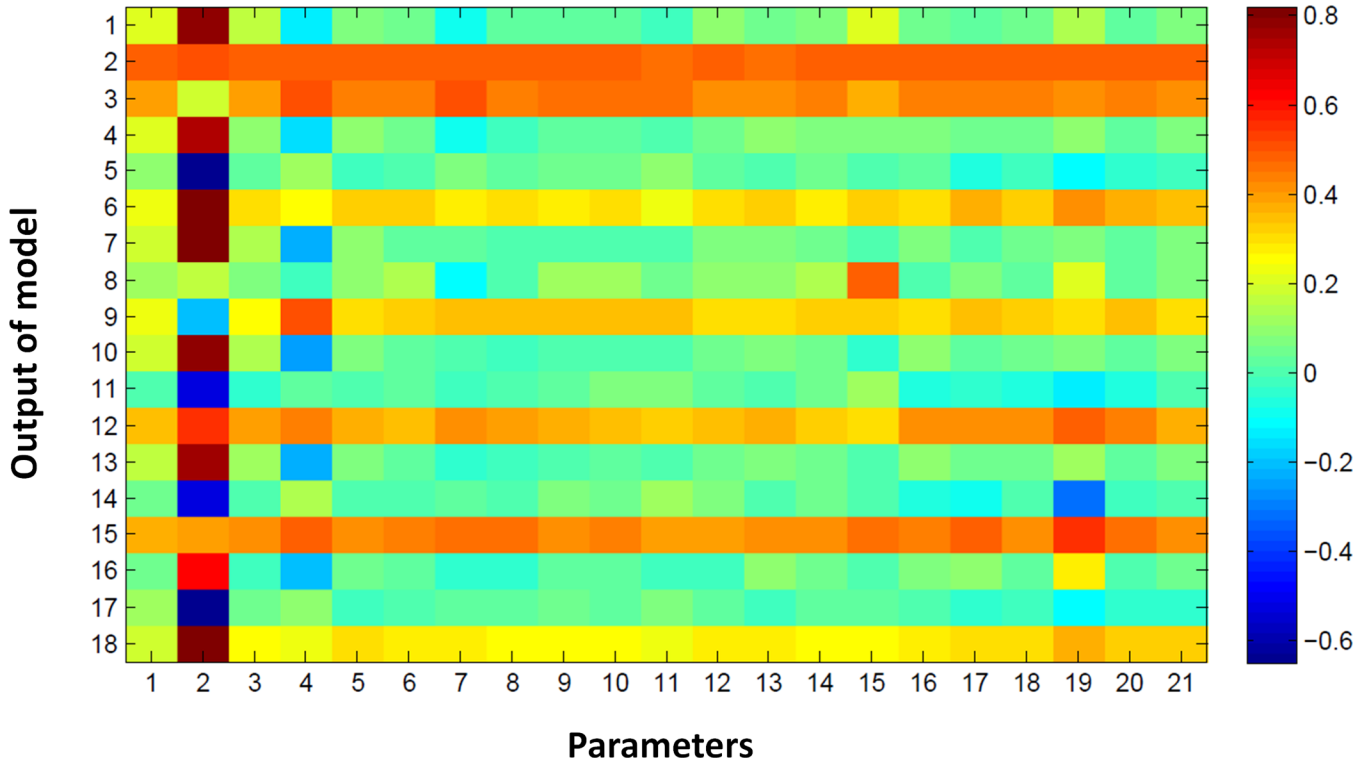

Fig. 5.

Theoretical results from function analysis of parameters in the model. The heat map shows the results of Pearson correlation coefficients (PCCs) between total 21 model parameters and total 18 system outputs.

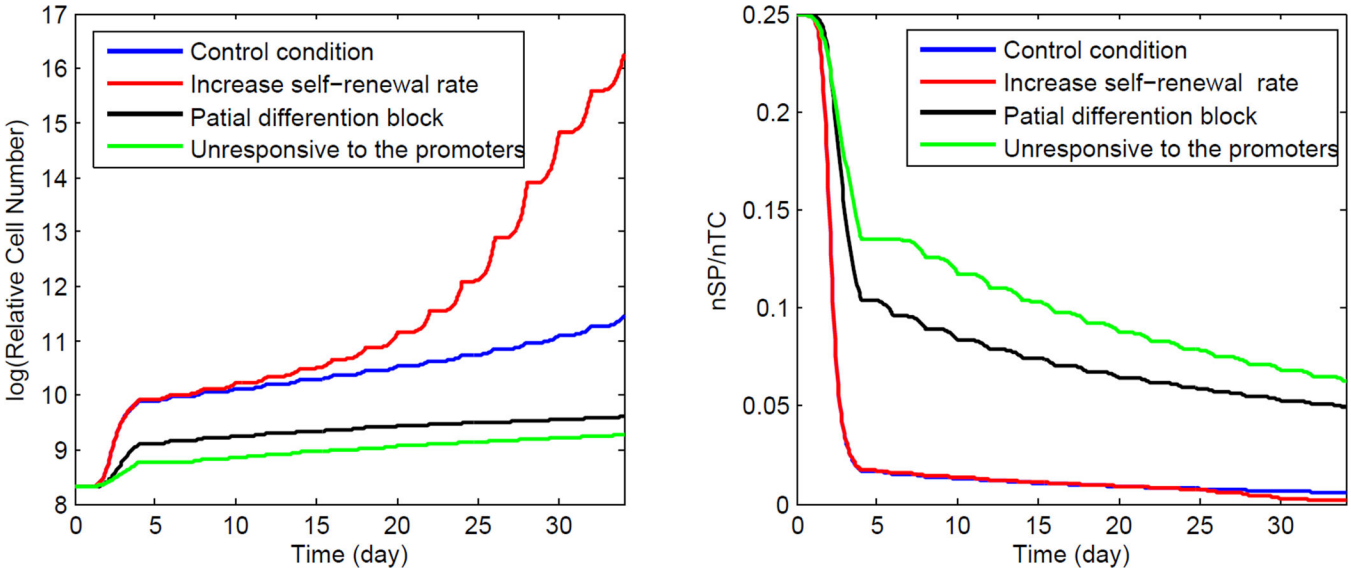

Fig. 6.

Theoretical results from model under various treatment conditions. (a) The results of total cell number dynamics. (b) The results of the percentage dynamics of SP cells over total cells. “Increase self-renewal rate”: increasing f_{max} by 50%; “Partial differentiation block”: decreasing μ_{max} by 50%; “Unresponsive to the promoters”: setting SSF1 = SSF2 = 0.

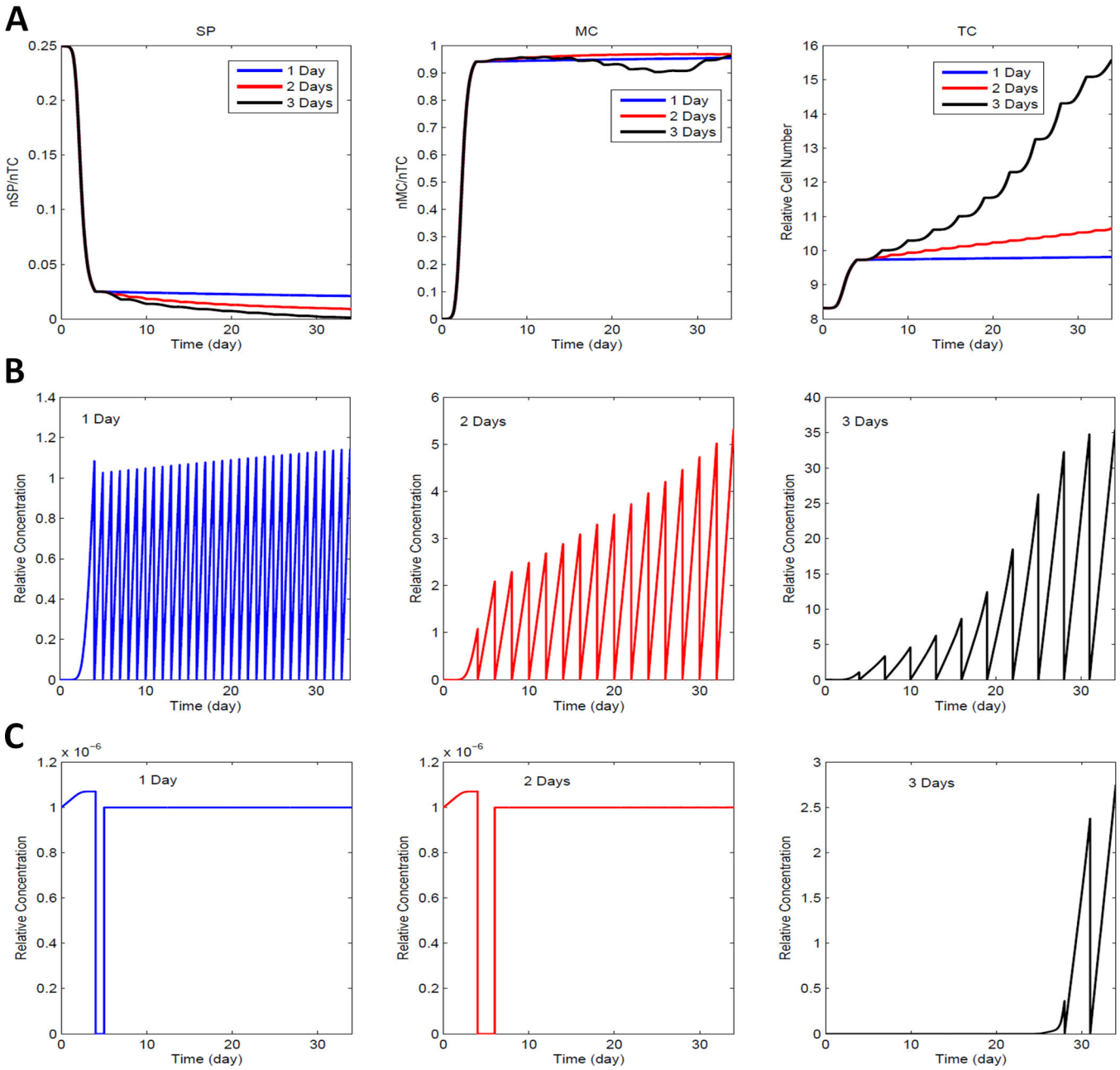

Fig. 7.

Theoretical results from model under various culture strategies. Three culture strategies were simulated based on the established linage model by renewing the medium at different frequency of culture manipulations, i.e., “1 Day”, “2 Days”, and “3 Days”. (a) The percentage dynamic of SP cells over total cells, the percentage dynamic of MCs over total cells, and the dynamic of the total cell population. (b and c) The concentration dynamics of ISF1 and ISF2.

TABLE I

Model Parameters and Coefficients of Variation

Parameters	Description	Units	LB	UB	Estimate	CV
f_{max}	Maximal self-renewal probability	--	$10^{-0.2}$	10^{0}	0.7904	0.1914
n_{max}	Compartment with maximal proliferation	--	$10^{0.2}$	$10^{1.1}$	11	0.1088
D_{SR}	Self-renewal decay term	--	10^{0}	10^{1}	12	0.1834
D_{GR}	Proliferative decay term	--	10^{0}	10^{1}	1.3137	0.8762
L_S	[ISF1] inducing ½ maximal ISF2	pg/ml	10^{0}	10^{2}	80	0.5493
K_S	Hill coefficient for ISF1 (in (7))	--	10^{-1}	10^{1}	7.1456	0.8778
μ_{max}	Maximal proliferation rate of CPC	day^{-1}	10^{-1}	10^{2}	50.4733	0.7898
μ_{+}	Maximal proliferation rate of MC	day^{-1}	10^{-1}	10^{2}	0.0812	1.0201
sr_1	Secretion rate of SSF1	pg/cell.d	10^{0}	10^{1}	11.9545	0.5029
sr_2	Secretion rate of SSF2	pg/cell.d	10^{0}	10^{1}	1.0027	0.5327
sr_3	Secretion rate of ISF1	pg/cell.d	10^{-1}	10^{1}	0.4442	0.5576
sr_4	Secretion rate of ISF2	pg/cell.d	10^{-1}	10^{1}	4.8639	1.2503
k_1	Hill coefficient for SSF1	--	10^{-1}	10^{1}	0.1807	0.9397
k_2	Hill coefficient for SSF2	--	10^{-1}	10^{1}	1.0894	1.2738
k_3	Hill coefficient for ISF1 (in (10))	--	10^{-1}	10^{1}	0.3503	0.7625
k_4	Hill coefficient for ISF2	--	10^{-1}	10^{1}	1.2584	0.7664
d_1	Hill coefficient for MC	--	10^{0}	10^{5}	107074.5	0.8651
d_2	Hill coefficient for CPC	--	10^{0}	10^{5}	120000	0.5797
D_1	MC inducing ½ maximal SFs secretion	pg/ml	10^{-1}	10^{1}	1.2356	0.7413
D_2	CPC inducing ½ maximal ISF2 secretion	pg/ml	10^{-1}	10^{1}	5.1167	1.4051
d_{MC}	Degradation rate of MC	pg/cell.d	10^{-6}	10^{0}	5.76×10^{-5}	2.1378

LB, lower bound; UB, upper bound; CV, coefficient of variation; The parameters whose CVs are highlighted with red (more than 1) are considered to be nonidentifiabie.